10th AIAA/ISSMO Multidisciplinary Analysis and Optimization Conference
30 August - 1 September 2004, Albany, New York

AIAA 2004-4553

Fuzzy Pareto Frontiers in Multidisciplinary System Architecture Analysis

Rudolf M. Smaling*
Massachusetts Institute of Technology, Cambridge, MA, 01730
Arvinmeritor, Columbus, IN, 47201

Olivier L. de Weck†
Massachusetts Institute of Technology, Cambridge, MA, 01730

This paper introduces the concept of fuzzy Pareto frontiers stemming in part from uncertainty in the analysis of concept system architectures in the context of new technology insertion into an existing complex system. The general approach in analyzing the system design or architecture trade-offs in the multi-disciplinary, multi-objective analysis is by generating a set of non-dominated solutions or Pareto frontier. The authors suggest in this paper that near-Pareto solutions should also be considered in the analysis. However, including Pareto and near-Pareto solutions in the analysis may be cumbersome due to the potentially large number of solutions. A filtering scheme is proposed to further reduce the set of solutions that include Pareto and near-Pareto points, by explicitly linking the objective space solutions to the originating design space.

Nomenclature

IC	Internal Combustion
BSFC	Brake Specific Fuel Consumption.
$BSNO_x$	Brake Specific NO_x
cr, r_c	Compression Ratio
γ	Ratio of specific heats
φ	Equivalence ratio
λ	Lambda (inverse of φ)
α	Fraction of reformer gas thermal energy into the engine
dsize	Fractional engine volume
Rp	Fuel fraction reformed
NO_x	Nitrogen Oxides
egr	Exhaust Gas Recirculation
O/C	Oxygen to Carbon Ratio
$\eta_{i,f}$	Indicated fuel conversion efficiency
FTP	Federal Test Prcedure
US06	United States supplemental test procedure
BMEP	Brake Mean Effective Pressure
FMEP	Friction Mean Effective Pressure
IMEP	Indicated mean effective pressure

* PhD Candidate, Engineering Systems Division, 3 Mudge Way, Bedford, MA 01730
* Director, Hydrogen Center of Competence, Air & Emissions Technologies, 950 W 450S, Columbus, IN 47201
† Robert N. Noyce Assistant Professor of Aeronautics and Astronautics and Engineering Systems, 77 Massachusetts Ave., Bld. 31, room 410

p_{amb}	Ambient pressure
p_i	Intake pressure
S_p	Piston speed
n_v	Number of valves per cylinder
r_i, r_e	Intake and exhaust valve radius respectively
WOT	Wide open throttle
Ta	Adiabatic temperature
E_{in}, E_{out}	Energy in and out respectively
Cp	Constant pressure specific heat
Cv	Constant volume specific heat
$Q_{combustion}$	Combustion energy released
Q_{lhv}	Lower heating value

I. Introduction

At the origin of most of today's complex engineering systems stand a handful of pioneers that acted as the designer, chief resource in engineering and manufacturing, entrepreneur, and founder of enterprises enduring until this day – the Wright brothers, Henry Ford, Karl Benz, Gottlieb Daimler, Glenn Curtiss, Louis Breguet are some of them. Since those early days, the design of complex systems such as air and space craft as well as automobiles has become highly specialized in the engineering disciplines. This specialization often is reflected in organizational design as well, where engineering disciplines are divided in functional domains with poor communication between them. As a result, sub-optimal solutions to performance requirements are often pursued by improper balancing of objectives across disciplines, primarily because the trade-offs between the disciplines are not well understood.

Multidisciplinary Design Optimization (MDO) has evolved over the last two decades as a result of the expressed need to "take a systems approach" in designing complex engineering systems as well as to better understand the inevitable trade-offs. While the origin of MDO lies in the aeronautics/astronautics field, the last decade has seen the methodology break through in other fields as well. The MDO framework is particularly attractive to systems architecting and concept selection. A number of quantitative concept selection methods have been proposed over the last decade. Some of them are axiomatic design[1], decision matrices[2, 3, 4], Utility function methods[5], and quality function deployment[6]. MDO has been used by some researchers to perform concept selection by posing the design as an optimization problem, then choosing the designs that satisfy the optimization conditions. Recently, some papers been published where the basic MDO framework is extended into concept or system architecture analysis and selection. Smaling[7] and Messac et al[8, 9, 10] developed the concept of system architecture selection using Pareto analysis. Computational cost constraints often limit model fidelity in MDO. This is not an issue with system architecture modeling since frequently only limited information is available, especially when new technologies are involved. A significant issue in modeling and analyzing system architecture and conceptual design is one of relevance and meaning. While it is safe to say that solution accuracy is almost impossible to ascertain, let alone achieve, the question is whether the results are meaningful under high levels of uncertainty. As such, the efforts underlying this paper are not so much intended to find an "optimal" solution, but rather to explore the system architecture design and objective space. To do so in a manner that will educate the system architect as to the behavior of the system resulting from the exploration of architecture design options. Work by de Weck[11] was stimulated by a similar sentiment: we are not necessarily interested in the best technical performance, but rather an optimal combination of technical and economic performance, which not necessarily is the same as the best system architecture based on technical merit alone.

It is also important for the reader to understand that generally in academic pursuits of new methodologies simple problems are used to illustrate the application of a particular methodology. The primary purpose is to develop new methodologies and use the simple problems that are universally understood, regardless of the audience's particular technical background, to explain the merits of the new methodology. Real engineering problems however tend to exhibit complexities that are difficult to deal with and are often only understood by a small subset of the audience, a primary reason most academicians tend to shy away from using them. However, as this paper intends to convey, important lessons can be gleaned from working with more complex problems.

II. Technology Background

Increased tension in the middle-east and resulting oil market uncertainty is driving transportation fuel prices to new highs. The transportation sector accounts for approximately two thirds of the oil consumed in the United States and cars and light duty vehicles account for a major portion of oil consumption within the transportation sector. There is also mounting evidence that the transportation sector is a significant contributor to the global climate changes witnessed over the last few decades. Both these issues underscore the need for increased urgency in developing automotive technologies to reduce oil consumption. Improvements in the average efficiency of cars and light duty vehicles can significantly reduce US oil consumption and the resulting dependence on foreign oil sources. Moreover, greenhouse gas emissions would also decrease. At the same time however, fuel economy improvements must not come at the expense of human health effects. For example, the European initiative to promote the use of diesel engines significantly increases fleet emissions of particulate matter and smog causing NO_x.

In order for a new technology to have a significant impact on either fuel consumption or greenhouse gas emissions, it must be of sufficient economic attractiveness to assure widespread adoption. With more than 200 million vehicles on the road in the US alone, even 100% adoption of a technology in new vehicles would take at least a decade to show its full impact.

US government support for new automotive technologies has emphasized the development of fuel cell vehicles. However, fuel cell vehicle technology and infrastructure requirements severely limit the prospects for widespread implementation of economically competitive vehicles in the foreseeable future.

The US passenger car fleet is largely powered by relatively low tech gasoline engines, hard to beat for their low cost and capability to comply with the strictest emissions standards in the world. The "European solution" does not make economic sense for the US. Even if the significant technical hurdles to comply with US emissions regulations can be overcome for diesel engines, the cost differential between gasoline and diesel engines would be such that the payback period exceeds the life of the vehicle.

A new approach that holds promise to significantly reduce national fuel consumption and greenhouse gas emissions and do so in an economically attractive manner is a hydrogen enhanced internal combustion engine. The plasma fuel reformer at the heart of this concept delivers a gaseous mixture containing hydrogen and carbon monoxide that enables both an extension of the charge dilution limit as well as significant engine knock attenuating properties[12,13]. It has been shown[14,15,16,17] that only a small fraction (20-30%) of the fuel going into the engine needs to be reformed into hydrogen rich gas in order to gain significant benefits.

Hydrogen addition affects combustion in an internal combustion engine in several ways. First of all, hydrogen addition can significantly increase flame speed. Flame speed is a primary factor in defining the lean limit - excess air slows down the combustion process to the point of not completing combustion in the time given during the power stroke. Effectively, hydrogen can extend the lean limit by off-setting the reduction in flame speed due to excess air. Secondly, recent work has shown that a hydrogen rich gas can enhance the octane rating of the overall cylinder mixture. This finding has the potential for increasing compression ratio, leading to direct gains in engine efficiency. Figure 1 and 2 illustrate the effect of hydrogen addition and how new system architectures emerge by the shifting of constraints.

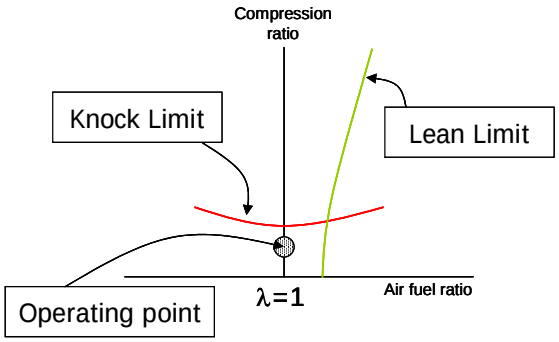

Figure 1: Conventional system

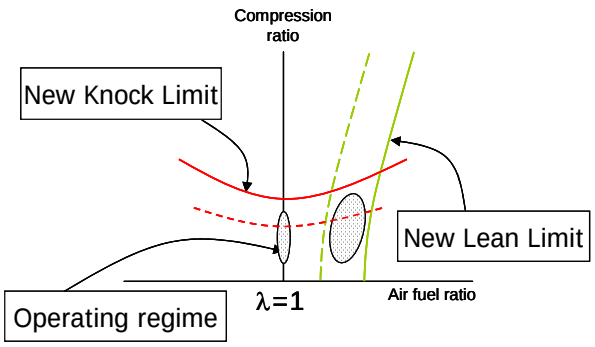

Figure 2: Emerging options due to technology insertion

Gasoline engines have two major operational constraints, namely the "knock limit" and the "lean limit" of combustion. The first constraint generally exhibits itself on a gasoline powered vehicle by a light pinging sound from the engine as one accelerates the vehicle. Excessive knock is destructive to the engine pistons and will lead to rapid engine failure. Passive knock control is built into the internal combustion engine by limiting the compression ratio of the engine. Many high performance engines will increase compression ratio to get higher engine power output, resulting in the need for high octane fuel. As mentioned, hydrogen rich gas from the plasma fuel reformer acts as an octane enhancer and therefore allows for a higher compression ratio, resulting in either greater power output or greater engine efficiency. To explain the benefits of extending the lean limit of combustion, see figures 3, 4, and 5 for illustration. The major regulated pollutants from internal combustion engines are hydrocarbons (HC), carbon monoxide (CO), and nitrogen oxides (NO and NO_2, or NO_x).

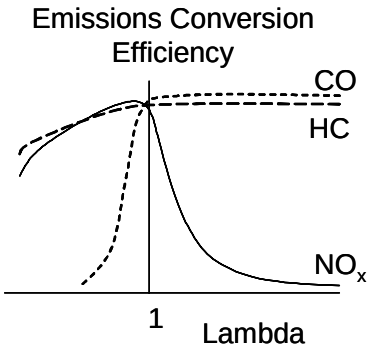

Figure 3: Catalyst performance

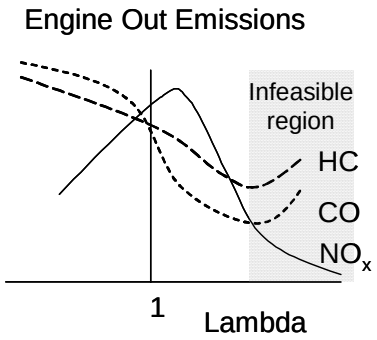

Figure 4: Engine out emissions

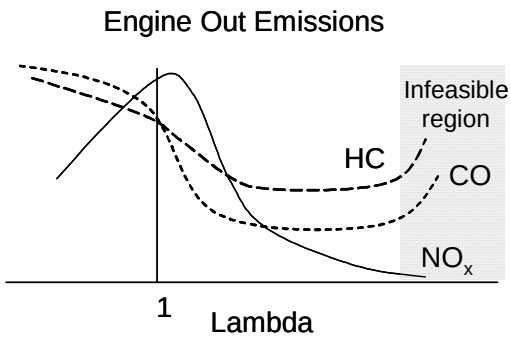

Figure 5: Emissions with lean limit extension

Figure three shows the typical conversion performance of an automotive catalytic converter for the three pollutants. It should be clear from this figure that only operation at lambda 1, meaning stoichiometry or the exact ratio of fuel and air where both the fuel and oxygen are completely consumed in the combustion reactions, ensure high enough conversion efficiencies to bring tailpipe emissions down low enough to meet regulations. While gasoline engines can be operated lean of stoichiometry and thus reduce engine out emissions and gain fuel consumption benefits to boot, combining figures 3 and 4 should lead one to conclude that tailpipe NOx emissions would be too high. The effect of extending the lean limit of combustion on engine out emissions is shown in figure 5. While the impact on HC and CO emissions is negligible, NO_x emissions continue to decline to near zero levels, not requiring any conversion performance from the catalytic converter. In essence then, the addition of a hydrogen rich gas from the plasma fuel reformer enables extremely lean engine operation, resulting in improved engine efficiency and significantly reduced engine out emissions levels. The challenge in implementing the new technology lies in the architecture one chooses to implement, which becomes a study of trade-offs well suited to multi-disciplinary analysis methodologies.

III. System Architectures

Significant extension of the dilution and knock limits of a homogeneous charge spark ignited IC engine opens up a number of possible new operating regimes. Each of the possible operating regimes will require specific engine and control system modifications as well as changes or additions in auxiliary hardware. The methodology followed in this study:

1. Enumerate all possible architectures for a hydrogen enhanced IC engine
2. Reduce the set of possible architectures to a feasible set
3. Develop computational sub-system models for the feasible set of architectures
4. Utilize the sub-system models to generate BSFC and $BSNO_x$ maps given the variations in multiple input variables
5. Insert BSFC and $BSNO_x$ maps into ADVISOR to generate vehicle emissions and fuel consumption data for a vehicle over various drive cycles.
6. Analyze the resulting data in the emissions versus fuel consumption versus system add-on cost design space

Possible System Architectures

The architecture concepts are developed by enumerating all the possible combinations of the attributes in table 1. At this phase of the architecture concept development stage, primary attention is given to high level operational features, without concern as to the implementation in hardware and software.

Naturally aspirated engine	Boosted engine
"Normal" compression ratio	"High" compression ratio
Air dilution	EGR dilution
Maintain engine size	Reduce engine size (increase power density)

Table 1: High Level Architecture Attributes

A discussion of the attributes follows:

1) A hydrogen enhanced IC engine can be operated in either naturally aspirated or boosted mode. In naturally aspirated mode, some efficiency and engine out NO_x emissions benefits can be obtained at a moderate cost. The primary reason the benefits are limited is due to the fact that at higher loads the dilution rate must be reduced to maintain engine power density. To maximize the benefit of hydrogen enhanced homogeneous burn SI combustion, some form of boosting must be considered in order to maintain dilution rates at higher loads. However, this will also come at a potentially significantly higher cost.

2) Increasing compression ratio has long been known to benefit engine efficiency. For gasoline engines however, engine knock constraints result in a practical limit for the compression ratio around 10:1 depending on fuel octane rating. Engine testing has shown that significant increases in compression ratio are possible when reformed fuel gas is added to the cylinder charge due to the knock attenuating properties of hydrogen and carbon monoxide.

3) To dilute the stoichiometric engine charge, there are two options: dilute with air or EGR. Dilution with air has greater benefits on fuel efficiency due to greater volume flow compared to EGR thus having a greater impact on reducing engine pumping losses at part load operating conditions. It also results in a more favorable working fluid from a thermodynamic perspective (greater ratio of specific heats). Choosing air as the diluent however, forces one to run the engine extremely lean in order to eliminate engine out NOx since catalytic treatment of NO_x in an oxygen rich environment is difficult and expensive. EGR dilution is the "safer" option, because if the target engine out NO_x levels cannot be reached, a simple three-way catalyst will eliminate the remaining NO_x downstream of the engine.

4) Once an IC engine is boosted, specific power output of the engine can be manipulated by controlling the boost pressure. The implication is that an engine of some size can be downsized significantly without sacrificing engine power output. Again, issues of implementation are not considered here. For example down sizing of a boosted gasoline engine typically results in unacceptable torque performance at low engine speeds. It is assumed in this study that technologies will be available to address that issue (e.g. electric assist turbo charging). The benefits are multiple:

i) Engine friction as a fraction of power output is significantly reduced.

ii) A smaller engine reduces weight of the vehicle and thus also provides indirect fuel savings.

iii) A smaller engine requires less space under the hood, enabling the engine compartment to be downsized.

However, increases in specific power also require reductions in compression ratio due to increased tendency for knock.

Feasible System Architectures

Enumerating all the possible combinations of the 4 attributes listed in table 1, leads to 16 possible architectures. However, many of those combinations are either not practical, or simply undesirable for a number of reasons. A reduced set of feasible options is shown in table 2:

Option 1	Option 2	Option 3	Option 4	Option 5	Option 6
Naturally aspirated	Naturally aspirated	Boosted	Boosted	Boosted	Boosted
Normal compression ratio	Normal compression ratio	Normal compression ratio	High compression ratio	Normal compression ratio	Normal compression ratio
Air dilution	EGR dilution	EGR dilution	Air dilution	Air dilution	EGR dilution
Normal size	Normal size	Normal size	Normal size	Downsized	Downsized

Table 2: Reduced set of feasible architecture options

IV. System Modeling

A multi-variable, multi-objective system modeling and analysis methodology is used to evaluate the architectures. A set of models was developed to describe the various aspects of interest for the system. All sub-models are written in MatLab to facilitate connectivity between the models and allow for optimization with respect to several objectives simultaneously. A description of some of the more important models follows:

Brake Specific Fuel Consumption

For the most part, the BSFC calculation methodology follows the one laid out by Shayler et al[18] with some modifications. Rather than assuming a value for the ratio of specific heats, γ, a cycle average γ is computed. This is a critical difference since in the proposed concepts the thermodynamic properties of the cylinder charge vary significantly from concept to concept. This can be seen as well from equation 1 for the ideal fuel-air cycle indicated fuel conversion efficiency (with cr = compression ratio):

$$\eta_{i,f} = 1 - \frac{1}{cr^{\gamma - 1}} \tag{1}$$

Engine Friction

An important part of the BSFC calculation is computing engine friction, which plays an important role especially in engine downsizing. Rather than follow Shayler[18], the methodology followed here is the one laid out by Wu and Ross[19]. They define 3 components of Friction Mean Effective Pressure:

The first part is a load dependent rubbing friction component relative to wide-open throttle (WOT):

$$FMEP_A = -6.898\left(\frac{p_{amb} - p_i}{p_{amb}}\right) + \left(0.088\, r_c + 0.182\, r_c^{\left(1.33 - 0.0238 S_p\right)}\right) \tag{2}$$

Where p_a and p_i are the ambient and intake charge pressures respectively, r_c is the compression ratio, and S_p represents piston speed. The second part is a load dependent intake and exhaust pumping friction component relative to WOT:

$$FMEP_B = \left(p_{amb} - p_i\right) - 4.12\,E^{-3}\left(\frac{p_{amb}^2 - p_i^2}{p_{amb}^2}\right)\left(\frac{S_p^2}{n_v^2 r_i^2}\right) - 0.178\,S_p^2\left(\frac{p_{amb}^2 - p_i^2}{p_{amb}^2}\right) - 4.12\,E^{-3}\left(\frac{p_{amb}^2 - p_i^2}{p_{amb}^2}\right)\left(\frac{S_p^2}{n_v^2 r_e^2}\right) \tag{3}$$

Where n_v represents the total number of valves per cylinder, and r_i and r_e represent the intake and exhaust valve radii respectively. The last part is a wide-open throttle friction component as written below. The constant values (78.5 and 5.1) have been adopted from GM 2.3L engine data scaled to a 1.9L engine. According to Wu and Ross, this part of the FMEP scales with $V_d^{-0.33}$.

$$FMEP_{WOT} = 78.5 + 5.1\left(\frac{N}{1000}\right)^2 \tag{4}$$

Total friction mean effective pressure can then be written as:

$$FMEP_{TOTAL} = FMEP_A + FMEP_B + FMEP_{WOT} \tag{5}$$

The plasma fuel reformer

A single step chemical reaction model is used to describe the plasma fuel reformer output based on input fuel and air flow. The latter is determined by specifying an oxygen-to-carbon ratio: O/C. For partial oxidation stoichiometry (i.e. the exact ratio of fuel and air leading to the ideal mix of only hydrogen, carbon monoxide and nitrogen) the value for O/C is unity. The model is constrained to O/C ratios between 1 and 3, the latter representing complete combustion. Below and O/C ratio of 1, carbon formation rises rapidly, which is undesirable. Between O/C ratios of 1 and 1.3, an additional factor is introduced to allow for the presence of small chain hydrocarbons. The factor is "tuned" to essentially make the model output similar to the output of laboratory prototypes of the

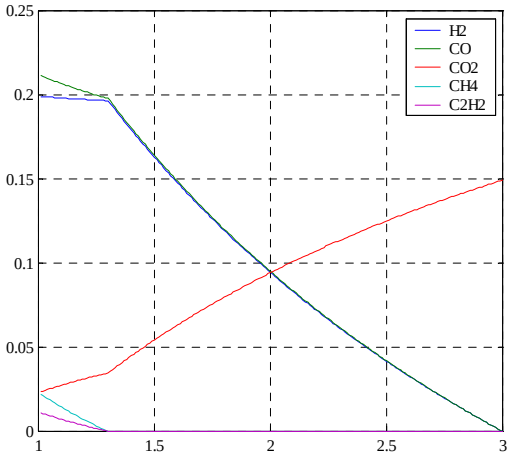

plasma fuel reformer. A typical plot of the output fractions of the plasma fuel reformer is shown in figure 6.

Figure 6: Plasma fuel reformer output versus input O/C ratio

In addition to computing the constituent concentrations in the reformed fuel gas, it is important to know the temperature of the reformed fuel gas. Using the lower heating values of both the input fuel as well as the out put gas constituents and their respective mass flow rates, one can calculate both the energy released as well as the energy efficiency of the reformer. The released energy during the partial oxidation process can be used to compute the adiabatic gas temperature at the exit of the fuel reformer (equation 6)

$$T_A = \frac{E_{in} - E_{out}}{\sum_{i=1}^{7}\left(C_{p_{\chi_i}} * \dot{m}_{\chi_i}\right)} + T_0 \tag{6}$$

with $\chi_i \in \langle H_2, CO, CO_2, H_2O, CH_4, C_2H_2, N_2 \rangle$

In the system analysis one can then analyze the impact of not cooling the reformed gas flow or cooling it which will affect both volumetric efficiency and NO_x emissions of the engine. There will be a cost penalty however for additional hardware in the form of a heat exchanger.

Dilution limit

Quantitative knowledge of where the dilution limit is located depending on the fraction of fuel reformed into hydrogen rich gas is required for this analysis to have any value in determining the benefits of hydrogen enhanced combustion. Tully[14,15] presents an array of single cylinder test data for various fuel fractions reformed –represented with synthetic gas replacing a fraction of fuel - while operating the engine with excess air. From his data, figure 7 was composed.

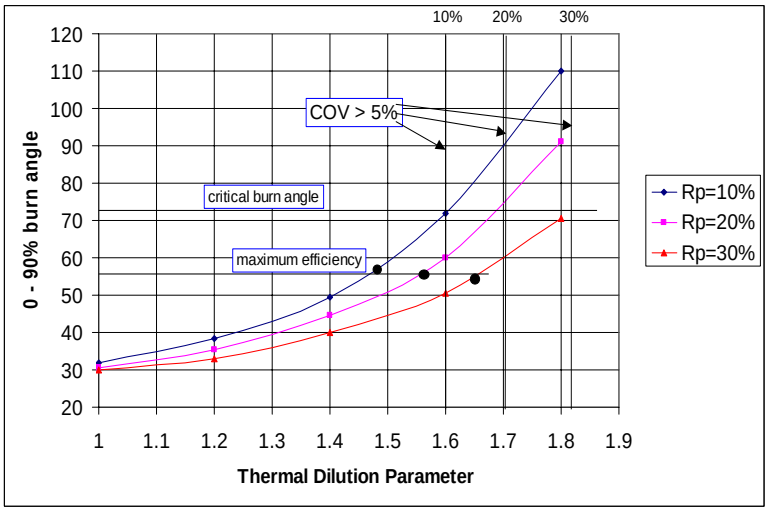

Figure 7: Burn duration versus thermal dilution parameter

The three curves represent the 0-90% burn duration versus a parameter called "thermal dilution parameter". Introduced by Tully, the thermal dilution parameter is the ratio of thermal gradient (during combustion) across the flame at stoichiometry over the thermal gradient during diluted combustion. The flame thermal gradient is essentially the same as the temperature rise due to combustion from the end of the compression stroke. Then:

$$\text{Thermal Dilution Parameter} = \frac{\Delta T_{stoichiometry}}{\Delta T_{dilute}} \tag{7}$$

Where ΔT can be written as:

$$\Delta T = \frac{Q_{combustion}}{\sum_{i=1}^{10}\left(\dot{m}_{\chi_i} * Cv_{\chi_i}\right)} = \frac{\sum_{j=1}^{5}\left(\dot{m}_{\chi_j} * Q_{LHV_{\chi_j}}\right)}{\sum_{i=1}^{10}\left(\dot{m}_{\chi_i} * Cv_{\chi_i}\right)} \tag{8}$$

with

$$\chi_j \in \langle C_7H_{14}, H_2, CO, CH_4, C_2H_2 \rangle$$

$$\chi_i \in \langle H_2, H_2O, CO, CO_2, C_7H_{14}, CH_4, C_2H_2, N_{2p}, N_{2e}, O_2 \rangle$$

The thermal dilution parameter is the most appropriate parameter to use in the analysis of diluted mixtures since it is the thermal gradient across the flame that directly drives flame propagation velocity and thus the course of combustion. Utilizing the thermal dilution parameter computed based on test data running with excess air, one can calculate equivalent EGR dilution rates. Additional testing has shown that the computed equivalent EGR rates match surprisingly well with actual test data.

Figure 7 furthermore shows both the points of "best engine efficiency" as well as the point where the covariance in the IMEP exceeds 5%. The latter generally defines the dilution limit. From figure 7, the following relations can

be derived for the Thermal Dilution Parameter as a function of fuel fraction reformed, resulting in peak engine efficiency as well as the dilution limit (where the covariance of IMEP reaches 5%):

$$TDP_{peak\_efficiency} = 1.387 + 0.875 * R_P \quad (9)$$

$$TDP_{dilution\_limit} = 1.49 + 1.1 * R_P \quad (10)$$

It stands to reason that the point of best efficiency occurs before one reaches the dilution limit. A sub-system model uses the data by creating a lookup table of fuel fraction reformed versus optimum air or EGR dilution rates, based on the underlying relationships to the thermal dilution parameter.

Compression Ratio

Topinka[12,13] has shown the knock attenuating properties of hydrogen and carbon monoxide when substituted for a fraction of the fuel into a spark ignited homogeneous charge IC engine. While her work, based on testing with primary reference fuels, suggests the possibility of increasing compression ratio by as much as 1 point for every 10% of fuel reformed, more recent testing with commercially available gasoline suggests that increase is about 0.5 points per 10% fuel reformed. The latter numbers have been used in the simulations presented here.

In addition to the more important sub-models explained here, there are many more details that go beyond the scope of this paper. The details of the system model employed can be found in reference 8.

Vehicle and drive-cycle model

In addition to the developed models, a freely available program was used called ADVISOR. ADVISOR, ADvanced VehIcle SimulatOR[20] developed by the National Renewable Energy Lab (NREL), is a set of model, data, and script text files for use with Matlab and Simulink. It is designed for rapid analysis of the performance and fuel economy of conventional, electric, and hybrid vehicles. ADVISOR also provides a backbone for the detailed simulation and analysis of user defined drivetrain components, a starting point of verified vehicle data and algorithms from which to take full advantage of the modeling flexibility of Simulink and analytic power of MATLAB. ADVISOR makes extensive use of maps based on empirical data to define various components of a vehicle drivetrain. Examples are Brake Specific Fuel Consumption or engine out emissions as a function of engine speed and torque. Two drive cycles have been used in this analysis: The Federal Test Procedure (FTP) and US06 supplemental drive cycle. The first is a relatively mild drive cycle with low engine speeds and torque. The latter is more aggressive with higher engine speeds and torque (figure 8). Average engine speed and torque for the FTP cycle are 1365 RPM and 27.7 ft.lbs respectively and 2347 RPM and 49.6 ft.lbs respectively for the US06.

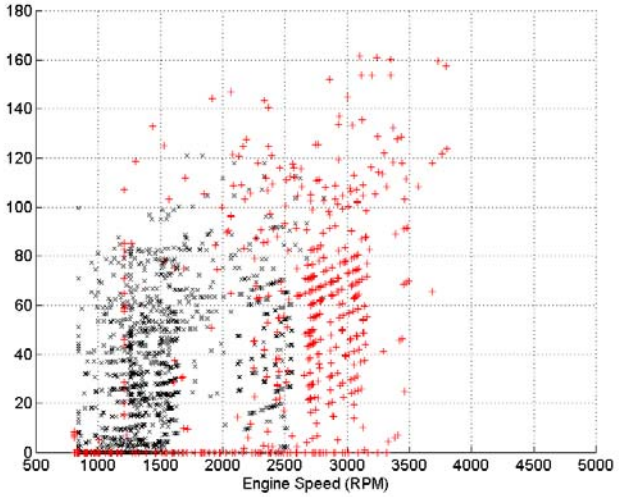

Figure 8: Engine speed and torque for the FTP (x) and US06 (+) drive cycles

The overall modeling framework is shown graphically in figure 9. While this type of framework is generally used in multi-variable, multi-objective *optimization* problems, it has been employed here more for *analysis* purposes. It was decided to explore the design space for a range of values for each of the components of the design vector. Especially at this stage of the design process it is desirable to analyze the broader design space, rather than focus on a small set of optimum values.

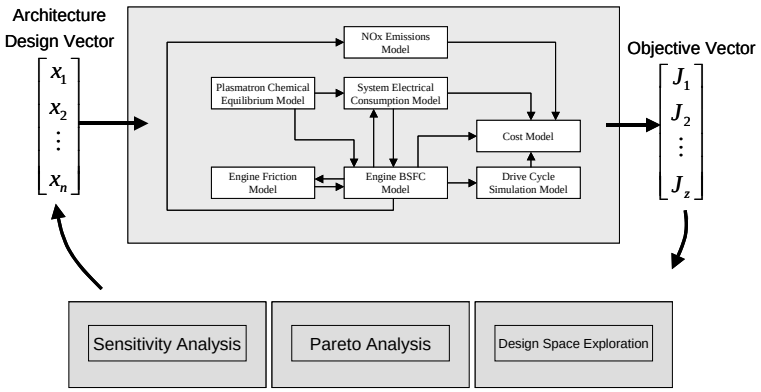

Figure 9: Architecture Modeling Framework

The Architecture design vector X contains 7 variables: X = [Rp, φ, egr, cr, o/c, α, dsize] while the Objective Vector contains the objectives of the analysis, namely fuel consumption (liters per 100 km), engine out NO_x emissions (gr/mi), and system add-on cost ($): J = [FC, NOx, C].

Model Validation

The developed system models were integrated and validated against an existing and validated model of a Saturn vehicle with 1.9L DOHC engine. The developed system model was set up to simulate an engine operating at stoichiometry with the fuel reformer "turned off". The resulting computed BSFC map is shown in figure 10 and can be compared against the actual (i.e. measured) BSFC map for this vehicle in figure 11.

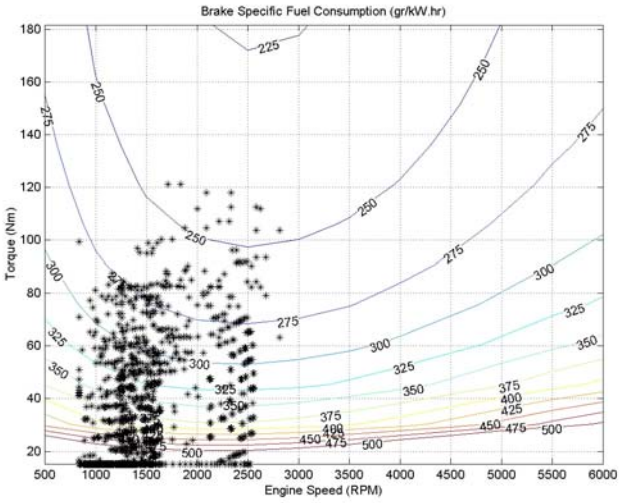

Figure 10: Computed BSFC map for Saturn 1.9L DOHC

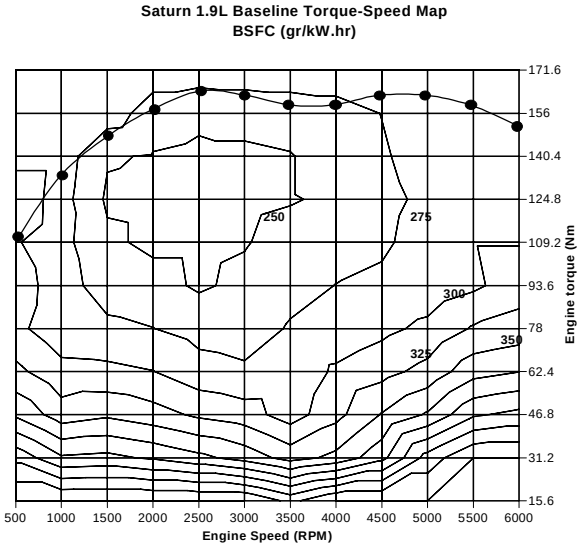

Figure 11: Measured BSFC map for Saturn 1.9L DOHC

V. System Architecture Simulation Results

One of the benefits of the modeling methodology applied in this work lies in the common framework allowing for direct comparison of simulation results for various architecture and system design options. Common design and objective vectors assure this to be true. Figure 12 compiles all simulation results for engine out NOx and fuel economy improvement in a single plot.

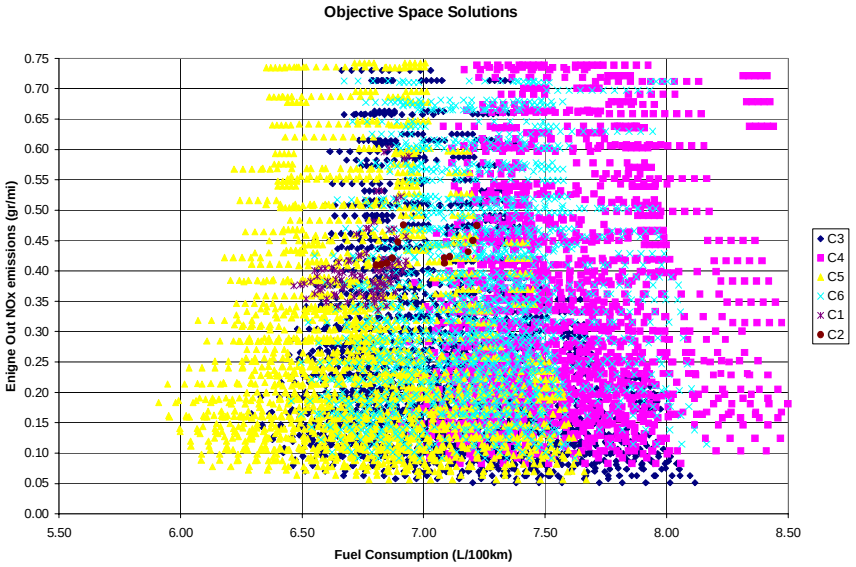

Figure 12: Concept comparison in the NOx versus Fuel Consumption objective space

From figure 12, one may quickly conclude that C5 (concept 5 or option 5 from table 2) is the superior architecture. Figure 12 however only shows two of the three objectives, namely the performance objectives of vehicle fuel consumption and engine out NOx emissions. Expected system add-on cost is not included for reasons of both propriety as well as the simple fact that uncertainty about the eventual cost impact of inserting this particular technology on a vehicle is very high. Nevertheless an attempt has been made to model the cost and the results have been incorporated in figure 13 in a normalized fashion. No actual cost numbers are shown – which would normally be plotted on a third axis – rather a normalized relative cost per unit fuel consumption improvement.

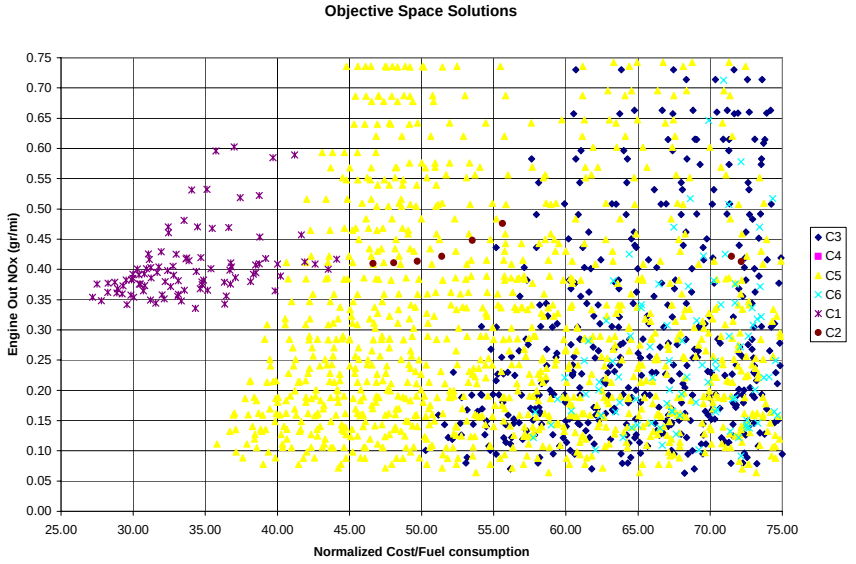

Figure 13: Concept comparison in the NO_x versus relative Cost/Fuel Consumption objective space

VI. System Architecture Analysis Methodology

The results shown in figure 13 indicate that when cost is taken into consideration, concept architecture 1 may be more cost effective, even if the overall fuel consumption improvement is much smaller than in the case of concept architecture 5. Additionally, emissions regulations vary worldwide. In the US for instance Tailpipe NOx emissions may not exceed 0.07 gr/mi, in Europe this number is 0.15 gr/mi. If engine out NOx emissions exceed regulations, a catalytic converter must be applied. If EGR dilution (i.e. concepts 2, 4, or 6) was selected, a simple three-way catalytic converter could do the job. In concept architectures 1, 3, and 5 however a very costly lean NOx catalysis system must be applied to further reduce engine out emissions, significantly affecting the cost/performance objectives. This simple analysis also ignores the fact that significant uncertainty may be contained in the data presented in figures 12 and 13 and one can therefore not just eliminate concept architectures 2,3,4, and 6.

To facilitate more detailed analysis of the simulation results, further data reduction is desired and a filtering scheme should be applied. In general, this would be achieved by generating the Pareto optimal set by eliminating all dominated points. A point $J^* = J(X^*)$ in the objective space Z is dominated if there exists another point J in the set Z such that $J \leq J^*$ with all $J_i < J_i^*$. X^* represents the point in the design space associated with J^*.

The Pareto optimal sets of system architecture options 1 through 6, based on the data presented in figure 12, is shown in figure 14.

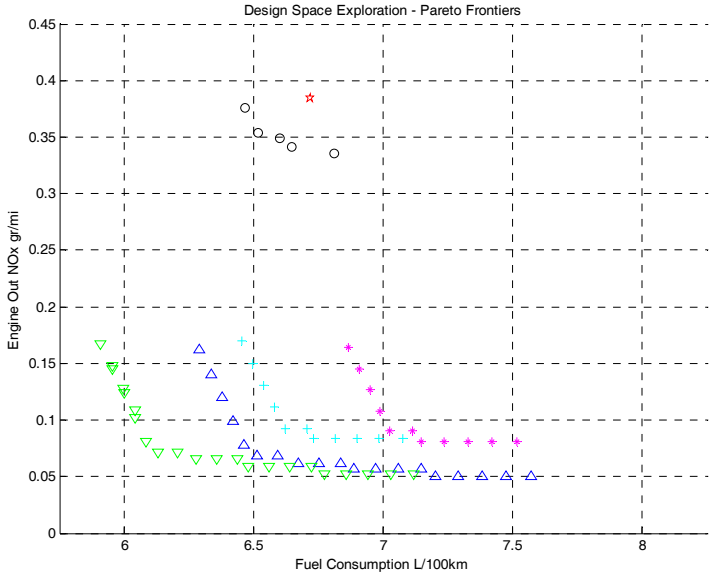

Figure 14: System Architecture Pareto Optimal Sets

However, it can be argued quite convincingly that this scheme goes too far in eliminating seemingly undesired solutions. If one can accept the argument that Pareto optimal solutions exhibit the lowest robustness of all the solutions in objective space Z, with increasing robustness – and decreasing uncertainty – away from the Pareto frontier, one would want to retain at least the near-Pareto solutions. This can be achieved readily by modifying the definition for the non-dominated points given in the previous paragraph:

A point $J^* = J(X^*)$ in the objective space Z is dominated by near-Pareto optimal solutions if there exists another point J in the set Z such that $(J+K) \leq J^*$ with all $(J_i + K_i) < J_i^*$. K represents the "slack" one seeks to introduce into the Pareto optimal set or the thickness of the (near) Pareto frontier for each component in the objective space.

The resulting set of "fuzzy" Pareto frontiers is shown in figure 15. By selecting the components of vector K appropriately, the analyst can include as many points as desired in the fuzzy Pareto frontier.

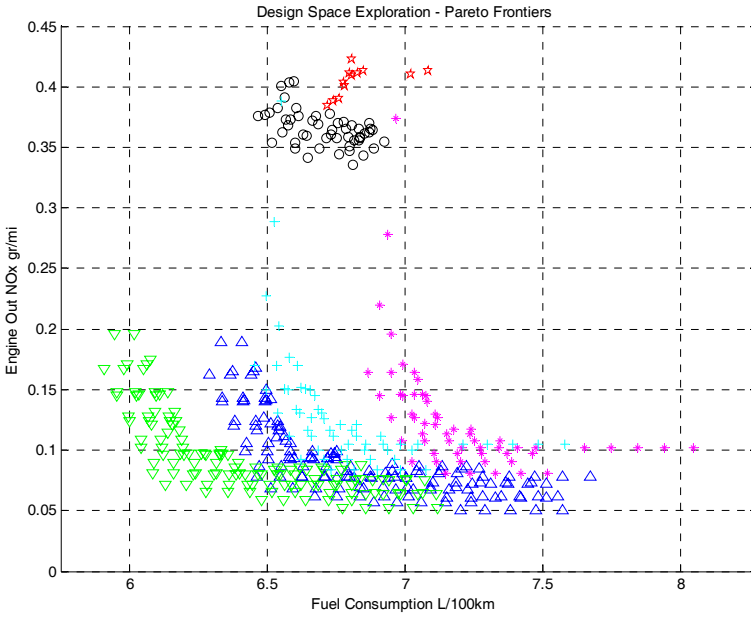

Figure 15: Pareto and near-Pareto solutions: Fuzzy Pareto frontiers

While eliminating of potentially valuable solutions can be avoided by generating the fuzzy Pareto frontier, the resulting sub-set of solutions Z* may be too large for additional processing and analysis. Messac et al[8,9,10] propose a scheme that eliminate points on the Pareto frontier based on their relative proximity to one another, i.e. out of every cluster of Pareto optimal solutions all but one point are eliminated. This elimination process however, is performed without regard for the relative proximity of the associated points in the design space. The authors of this paper argue that great care must be taken not to eliminate one of two or more points clustered in the objective space if the associated points in the design space are not clustered, as indicated in figure 16.

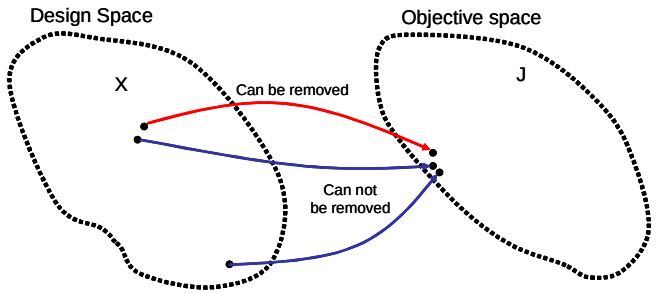

Figure 16: Addressing clusters

While with simple system problems this may not be an issue, more complex systems may exhibit clustering of points in the objective space, while their associated design points are not necessarily clustered. One must therefore take care in not eliminating potentially valuable architectures or designs at this stage of analysis.

To facilitate further filtering and analysis, the design vector X and objective vector J are normalized as follows:

$$J_i^{norm} = \frac{J_i - J_i^o}{J_i^{\max} - J_i^o} \quad \text{and} \quad X_i^{norm} = \frac{X_i - X_i^o}{X_i^{\max} - X_i^o} \tag{11}$$

Where J^o is the Utopia point, defined by $J_i^o = \min(J_i)$ and J^{max} represents the points where any one of the objectives reaches its maximum value on the true Pareto frontier, also called the anchor points.

One suitable filtering methodology may be to compute the cross-orthogonality between any two vectors in the objective space and their associated vectors in the design space. Using the Utopia point as the origin in the objective space and zero as the origin in the design space, a cross-orthogonality matrix is computed for each space as follows:

$$COM_X(a,b) = \frac{X^a * X^b}{\left|X^a\right| * \left|X^b\right|}, \text{ where X = [Rp, } \varphi\text{, egr, cr, o/c, } \alpha\text{, dsize]} \tag{12}$$

$$COM_J(a,b) = \frac{J^a * J^b}{\left|J^a\right| * \left|J^b\right|}, \text{ where J = [FC, NOx]} \tag{13}$$

Given the choice of points of origin for both the design and objective vectors, the cross-orthogonality between any two vectors X^a and X^b or J^a and J^b can take values between 0 (meaning the vectors are normal to one another) and 1 (meaning the vectors are aligned). With these two matrices computed, one can then compare the a^{th} and b^{th} point in both matrices simultaneously and eliminate either the a^{th} or bj^{th} point if the cross-orthogonality value is close to 1 in both design and objective space cross-orthogonality matrices (i.e. if both the a^{th} and b^{th} points in the design and objective space are clustered together, one can be eliminated):

In other words, *if* $COM_X(a,b) > \delta$ *and* $COM_J(a,b) > \varepsilon$, with δ and ε user definable scalar values, then either point a or b can be eliminated. One must take care however not to randomly eliminate one or the other point; there are several considerations to be made when two points in objective space and their associated points in design space are clustered together:

1) Whichever point in the objective space has the shortest distance to the Utopian point should be preserved.
2) The Pareto frontier anchor points should be preserved since they represent unique solutions.

The first can be addressed by computing the Euclidian distance of the a^{th} and b^{th} points in the objective space to the Utopian point:

$$D_a = \left\|J^a - J^o\right\| = \left\{\sum_{n=1}^{k}\left[J_n^a - J_n^o\right]^2\right\}^{1/2} \tag{14}$$

The second can be addressed by tagging those anchor points A^k for which any component k exhibits a minimum value. I.e. for an n-dimensional objective space there will be n anchor points.

If two points are found to be clustered in both objective and design space, then the one computed to be closest to the Utopia point will be preserved unless the other point is an anchor points.

Applying the proposed filtering scheme to the data represented in figure 15 will result in a reduced dataset. The designer now has the option to select the level of data reduction by appropriate selection of values for δ and ε. A reasonable reduction in data is shown in figure 17.

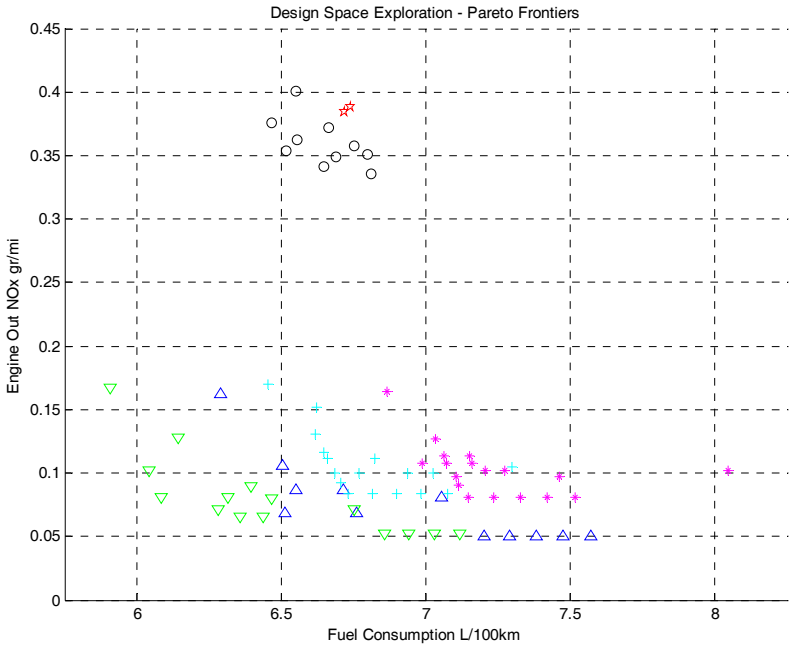

Figure 17: Filtered fuzzy Pareto fronts

To highlight the author's exertion that great care must be taken not to randomly remove points from data clusters in the objective space without considering the associated design space variables, let us take a closer look at a particular (randomly chosen) cluster in the concept 5 data (yellow points in figure 12, and green upside down triangles in figures 14, 15, and 17). All points in this particular cluster are shown by themselves in figure 18 and the associated design variables are shown in figure 19 in order 1-7: [Rp, φ, egr, cr, o/c, α, dsize].

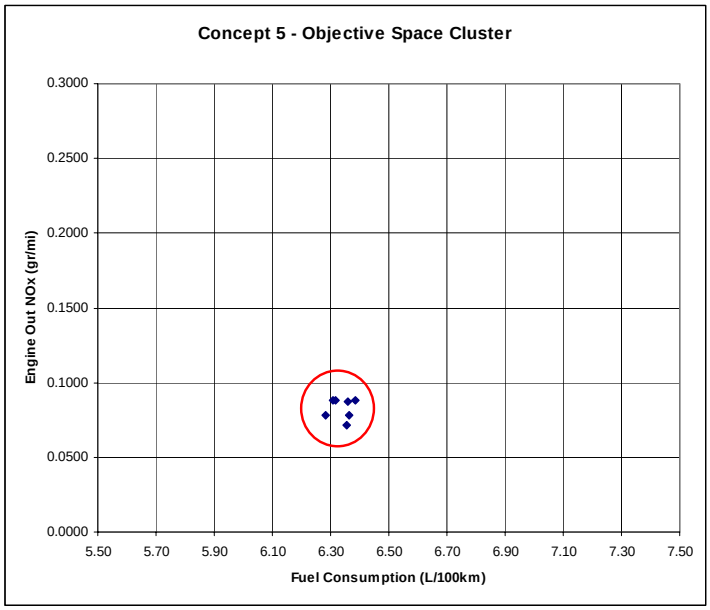

Figure 18: Objective Space Data Cluster

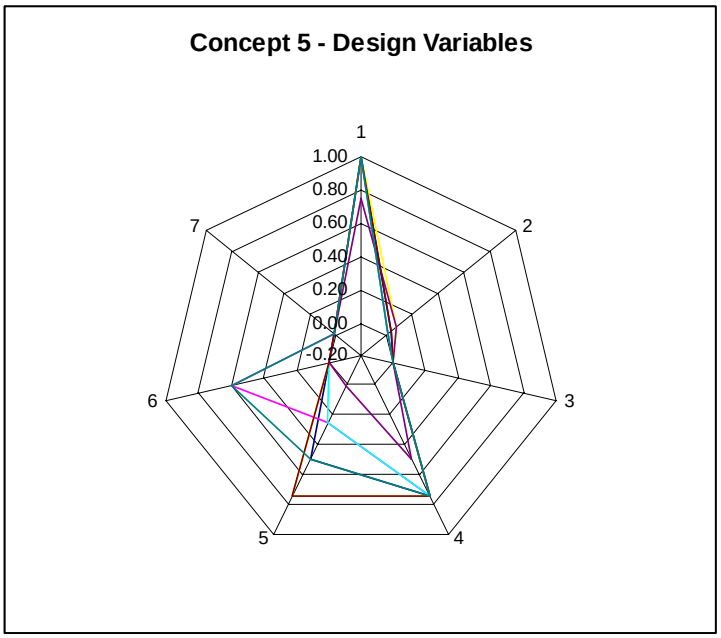

Figure 19: Design Space Associated Variables

While the cluster of data in figure 18 falls within 4% of the full range of fuel consumption data and within 2% of the full range of engine out NOx data, figure 19 shows far less clustering than that. After applying the proposed filtering scheme, figures 20 show the remaining points from the original cluster and figure 21 shows that it is justified to preserve three points – rather than randomly eliminating all but one - from the original cluster due to significant diversity in the associated design vector.

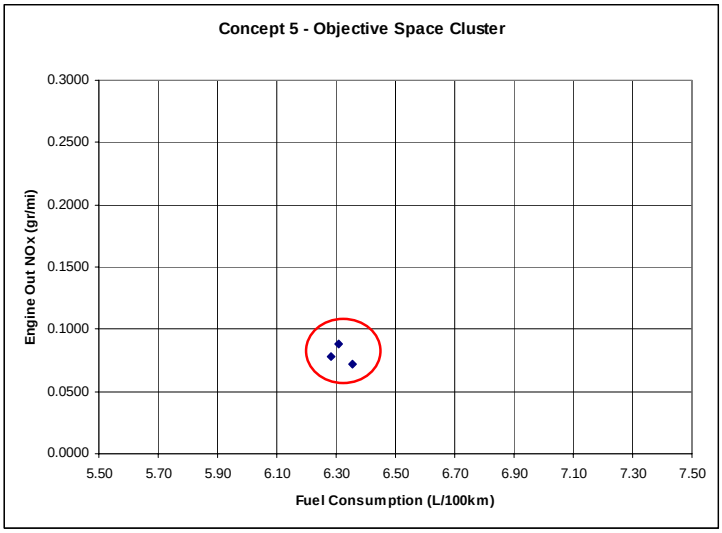

Figure 20: Filtered Objective Space Data Cluster

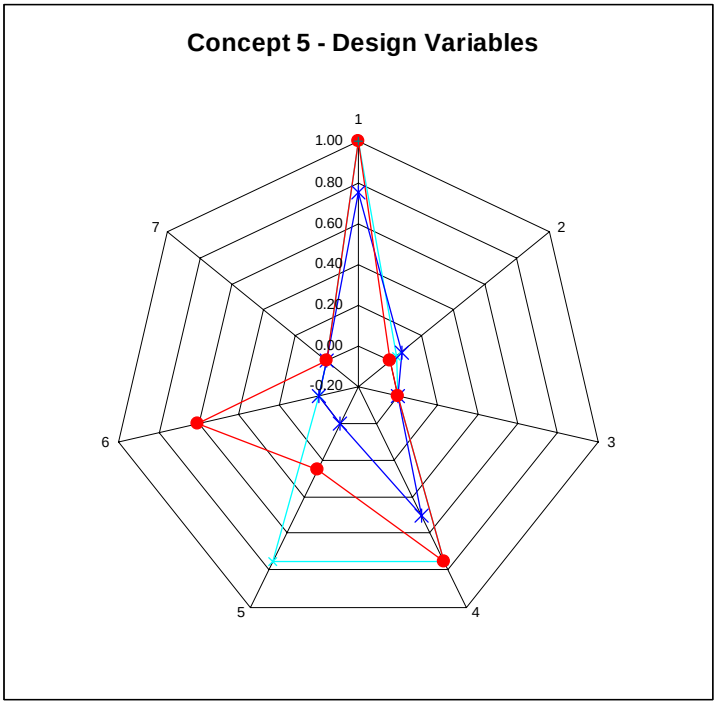

Figure 21: Design Space Associated Variables

In this particular example of cluster filtering, the two variables that vary significantly are those of O/C (5) ratio and alpha (6). The O/C ratio variable refers to the oxygen to carbon ratio in the fuel/air mixture entering the plasma fuel reformer. Without going into detailed reformer design issues, a larger value for the O/C ratio may have significant impact on design of the reformer. Similarly, alpha is important. It represents the amount of cooling of the reformed fuel gas is required before it enters the engine intake manifold. The difference between small and large values is the difference between requiring a heat exchanger or not, a significant issue for system cost.

VII. Conclusions and Future Work

In this paper a novel data reduction methodology is presented that preserves a level of richness in the design space that other methods do not seem to pursue or attain. The method incorporates the use of fuzzy Pareto frontiers and explicitly links the objective and design spaces to ensure that design space diversity is preserved in eliminating data clusters in the objective space. Critical to demonstrating the methodology is the use of a sample problem of far greater complexity than usually applied in the development of new methodologies.

An important reason for developing the concept of the fuzzy Pareto frontier is that model fidelity and other sources of uncertainty do not necessarily make Pareto optimal solutions “optimal”. Optimal solutions in terms of lower uncertainty or improved robustness may lie near the Pareto frontier. Future work will focus on the sources of uncertainty and attempt to quantify them within the present analysis framework.

VIII. Acknowledgments

This research was made possible with the support from Arvinmeritor corporation. Special thanks go to Professor John Heywood for helpful discussions and guidance in the modeling efforts. Special thanks also to John Grace for his support of this project and the research presented here.

IX. References

[1]Suh, N. P.: “The Principles of Design” New York: Oxford University Press 1990
[2]Ulrich, K. T. and Eppinger, S.D.: “Product Design and Development”, Boston: McGraw-Hill, Inc., 2000

[3]Magrab, E. B.: "Integrated Product and Process Design and Development: The Product Realization Process". New York: CRC Press, 1997
[4]Pahl, G. and W. Beitz: "Engineering Design: A Systematic Approach", London: Springer-Verlag, second edition, 1996
[5]Otto, K. N.: "Measurement Analysis of Product Design Methods". Research in Engineering Design, 86–101, 1995
[6]Magrab, E. B.: "Integrated Product and Process Design and Development: The Product Realization Process". New York:
[7]Smaling, R.M., "System Architecture Selection in a Multi-Disciplinary System Design Optimization Framework", MIT Thesis, Cambridge, MA, 2003
[8]Mesac, A., Mattson, C.A., "Development of a Pareto Based Concept Selection Method", AIAA 2002-1231, Denver, 2002
[9]Mesac, A., Mattson, C.A., "Concept Selection in n-Dimension using s-Pareto Frontiers and Visualization", AIAA 2002-5418, Atlanta, 2002
[10]Mesac, A., Mattson, C.A, Maria, A., "Multicriteria Decision Making for Production System Conceptual Design Using s-Pareto Frontiers", AIAA 2003-1442, Norfolk, 2003
[11]De Weck, O.L., "Multivariable Isoperformance Methodology for Precision Opto-Mechanical Systems" MIT Department of Aeronautics and Astronautics, 2001
[12]Topinka, J., "Knock Behavior of a Lean-Burn, Hydrogen-Enhanced Engine Concept," MIT Thesis, Cambridge, MA, 2003.
[13]Topinka, J.A., Gerty, M.D., Heywood, J.B., Keck, J.C., "Knock Behavior of a Lean-Burn, H2 and CO Enhanced, SI Gasoline Engine Concept", SAE 2004-01-0975, , SAE International Congress and Exposition, Detroit, MI, 2004.
[14]Tully, E. "Lean-Burn Characterisitics of a Gasoline Engine Enriched with Hydrogen from a Plasmatron Fuel Reformer", MIT Thesis, Cambridge, MA, 2002.
[15]Tully E., Heywood, J.B., "Lean-Burn Characteristics of a Gasoline Engine Enriched with Hydrogen from a Plasmatron Fuel Reformer", SAE 2003-01-0630, SAE International Congress and Exposition, Detroit, MI, 2003
[16]Lengweiler, A., "SI Engine Combustion and Enhancement Using Hydrogen from a Plasmatron Fuel Converter", MIT Thesis, Cambridge, MA, 2001.
[17]Ivanic, Z., "Predicting the Behavior of a Lean-Burn, Hydrogen-Enhanced Engine Concept", MIT Thesis, Cambridge, MA, 2004
[18]Shayler P.J., Chick, J.P., Eade, D., "A Method of Predicting Brake Specific Fuel Consumption Maps", SAE 1999-01-0556, SAE International Congress and Exposition, Detroit, MI, 1999.
[19]Wu, W., Ross, M. "Spark Ignition Engine Fuel Consumption Modeling", SAE 1999-01-0554, SAE International Congress and Exposition, Detroit, MI, 1999.
[20]http://www.ctts.nrel.gov/analysis/